

MULTI-DISCIPLINARY DESIGN OF HIGH-SPEED COMPRESSORS FOR PROSPECTIVE TURBO-SHAFT ENGINE

A.N.Startsev*, Yu.M.Temis*, Eu.G.Steshakov*, D.A.Yakushev*

*Central Institute of Aviation Motors, Moscow, RUSSIA

Keywords: *axial-centrifugal compressor, thermodynamic cycle, 3D Navier-Stokes solver*

Abstract

In order to obtain higher efficiency thermodynamic cycles in prospective turbo-shaft engine, overall pressure ratio (PR) and efficiency of its compressor must be increased. Moreover there is a problem of growth potential of a compressor to develop a family of engines with increasing shaft power.

This paper focuses on 3D Navier-Stokes aerodynamic design of a high pressure ratio compressors to identify compressor configuration, 3D blading and flow-path providing effective aerodynamics.

This paper describes some observations appearing in the aerodynamic design of high-speed compact axial-centrifugal compressors achieving $PR = 16 \div 25$ in $4 \div 6$ stages. Mechanical requirements are also taken into consideration.

In-house and commercial validated 3D numerical tools are used to assess the quality of the aerodynamic and strength design.

1 Introduction

The prospective turbo-shaft engine's trend towards higher power-to-weight ratio and reduced specific fuel consumption leads to aggressive designs: fewer compressor and turbine stages, higher pressure ratio and minimal axial length of bladed rows and spacing between them. Certainly, the prospective turbo-shaft engine requires higher adiabatic efficiency of its components.

High thermodynamic cycle parameters cause a number of technical challengers for compressor and engine design: aerodynamics of low corrected flow in aft stages, strength-of-material and cooling limitations at high compressor discharge temperatures, two-spool architecture and other construction complexities.

Nevertheless, actual design is a trade-off between level of complexity of compressor construction and its adiabatic efficiency.

As is known, 2000 ÷ 3500 shaft horse power (SHP) turbo-shaft engines are often constructed with axial-centrifugal compressor consisting of a number of axial stages terminated by centrifugal stage.

The principles of compression in axial stages and centrifugal stage are different. Single centrifugal stage achieves high compression through the large radius at the outlet of its impeller. In contrary, axial compressor consists of a number of stages of relatively lower compression and cumulates high compression stage-by-stage. Both types of compression have a common feature: the higher rotational speed - the larger compression. Nevertheless, at high rotational speed absolute supersonic flow velocity at the exit of centrifugal impeller and relative supersonic pre-shock flow velocity on tip of axial rotor are experienced. These events cause remarkable increase of total pressure losses and decrease efficiency.

For a given value of the overall pressure ratio one can redistribute compression between axial part and centrifugal stage of compressor to maximize adiabatic efficiency. Aerodynamic loadings of axial stages can be controlled to

provide desired compression characteristics across the compressor improving its efficiency.

Axial-centrifugal compressors discussed below are constructed of three, four and five axial stages and a centrifugal stage. For these compressors the following designations are used: 3+1, 4+1 and 5+1 correspondingly.

One of the most interesting practical questions is the development of a family of engines based on a well-developed engine-prototype. As an example of family development, FLIGHT INTERNATIONAL (25 April 1987, page 21) outlined General Electric's turbo-shaft T700 growth steps, and variation of parameters of T700 compressor. Designed as a 1,500SHP- class turbo-shaft, the original T700-700 in fact produced more than 1,600SHP. The 1,700SHP T700-401 represented the first growth step, achieved by increasing compressor airflow 3% and turbine temperature by 30°C. The 1,850SHP T700-401C represented the second stage of growth: with more-efficient centrifugal compressor (PR=17.1:1) and 1,370°C-class high-pressure turbine (improved blade materials, cooling and aerofoils). The third step (2,000SHP CT7-6) included 12% increased-airflow compressor with higher PR=18.4:1. Thus, GE achieved 20% increase of SHP with unchanged compressor architecture by means of 15% increase of flow-rate and 15% increase of PR.

In this paper a family of compressors is developed to investigate different aerodynamic design approaches and identify structural design limitations.

To provide continuous advances to achieve potential growth, aerodynamic design of 3+1, 4+1 and 5+1 compressors is organized as step-by-step "evolution" process: a family of compressors for a range of flow-rate (+25%) and total pressure ratio (16÷25) (to achieve 30% gain in shaft horse power) has been constructed starting with a 4+1 compressor-prototype. As a result, new compressors retain proven parameters of the prototype.

"Evolution" of 4+1 prototype to 3+1, 4+1 and 5+1 has been performed on the base of:

- the same RPM;
- the same hub contour of compressors;
- the same front axial stages (three stages);

- the same velocity triangles;
- addition or removal of axial stage (at the exit of axial part of compressor).

Rotor1(rotating bladed row of the 1st axial stage)'s tip rotational speed (U_{R1tip}) equal to 493m/s is adopted as a limiting value. This limiter can be characterized as "aerodynamic" and used to control shock losses in Rotor1.

Centrifugal impeller-exit tip speed (U_{2imp}) varies in the range 529÷593m/s, and is a "structural limiter" dependent on type of material and high temperature at the exit of impeller.

2 4+1 Compressor-Prototype

Prototype (in other words, reference compressor) consists of four axial stages with tapered-tip diameter flow path and a centrifugal stage (see Fig.1).

The compressor design point is PR=16:1 at the flow-rate $G_{corr}=4.75$ kg/s.

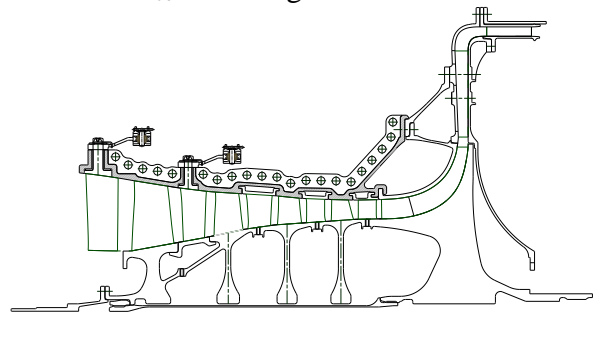


Fig. 1. Construction of the 4+1 Prototype

2.1 Axial Part of Compressor-Prototype

Inlet hub diameter is dictated by the level of torque carried by the power shaft and is an input parameter for aerodynamic design. Given flow-rate determines inlet tip diameter of the Rotor1. Corresponding tip speed U_{R1tip} equals to 456m/s. This tip speed is large enough to design "lightly loaded" 1st axial stage. (For a long time, concept of "lightly loaded front stage" is applied in the design of GE90 engine high pressure compressors.)

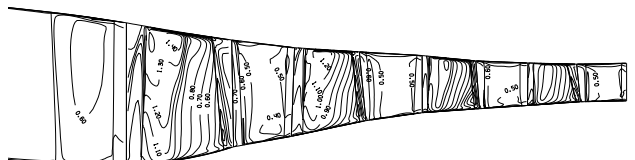


Fig. 2. Mach level lines on suction side of rotor blades

Fig.2 demonstrates that pre-shock Mach number on tip of Rotor1 is slightly more than 1.4. This value is acceptable since adiabatic efficiency of Stage1 is $0.85 \div 0.86$. Pre-shock Mach number on tip of Rotor2 is 1.2 and adiabatic efficiency of Stage2 is $0.885 \div 0.89$.

Cumulative parameters of three and four axial stages of the Compressor-Prototype are as follows:

$U_{Rtip} = 456 \text{ m/s}$	3 stages	4stages
Pressure ratio PR	4.40	5.74
Adiabatic efficiency η_{ad}^*	0.858	0.847

Axial compressor is designed for small-sized engine, therefore tip clearance over rotor of exit axial stage is $1.4 \div 1.6\%$ of the blade height, which greatly reduces the efficiency of the axial compressor.

The last axial stage's guide vane provides a certain amount of pre-swirl (in the direction of rotation) at the inlet of centrifugal impeller.

2.2 Centrifugal Stage of Compressor-Prototype

Centrifugal stage is the rear stage in axial-centrifugal compressor. Centrifugal stage plays a key role: it determines the operating point of the axial compressor and stability margin of the compressor as a whole. In addition, the compressor efficiency largely depends on the efficiency of the centrifugal stage. As known, centrifugal stage efficiency is always less than that of any axial compressor. Therefore, to obtain high efficiency of the axial-centrifugal compressor, work done by centrifugal stage (as a fraction of work done by the whole axial-centrifugal compressor) should be minimal.

Centrifugal stage works as a throttle for the axial part of compressor and it is useful to choose the impeller-inlet blade span so that the axial part of the compressor operates at maximum efficiency. Adiabatic efficiency of impeller consisting of main blades and splitters depends on the value of relative flow Mach

number realized in blade-to-blade channel: supersonic flow pockets are prohibited.

The impeller-exit blade height must provide the output flow angle less than 70° (otherwise, vaned diffuser's total pressure losses are increased considerably). The value of flow angle allows logarithmic spiral design of the diffuser vanes. Log-spiral vanes ensure viscous flow diffusion without separation. The only disadvantage is large (60°) flow angle to the outlet guide vanes. However, low level of Mach number at the exit of compressor provides high value of total pressure recovery.

As already mentioned, centrifugal impeller-exit tip speed does not exceed 593m/s. Reduction of the tip speed is more acceptable for structural design at higher operating temperatures. Maximum value of total temperature considered in this paper is 830K (corresponding to 27.5:1 total pressure ratio). This impeller discharge temperature is equal to 540°C and corresponds to the maximum limit of temperature operating range shown on Fig.6. Maximum allowable tip speed indicated on Fig.6 is less than 650m/s for a titanium-base alloy. Such type titanium-base alloy is currently available.

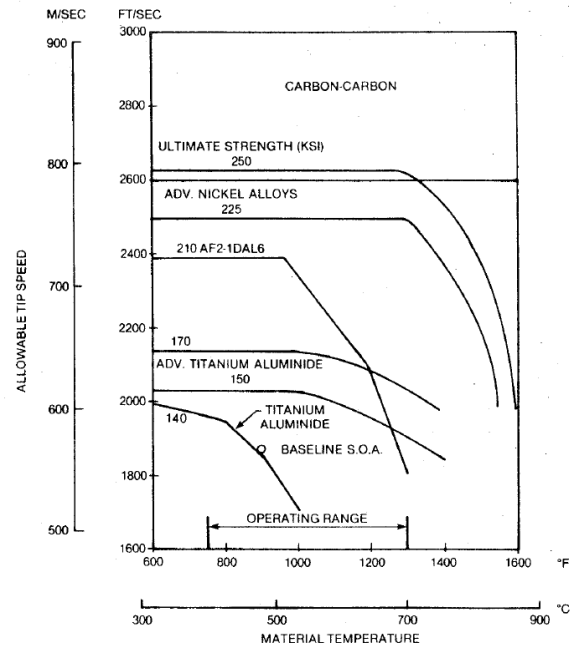


Fig. 3. Centrifugal impeller maximum allowable tip speed, taken from Singh, B., (1991), "Small Engine Component Study", NASA CR-175079, Teledyne CAE Report No 2224

2.3 Thermal and Structural Analyses

Feasibility of the rotor construction was verified with thermal and subsequent structural analysis.

Thermal conditions of axial blades and disks and impeller’s blades and disk are the result of conjugate problem solution: heat conduction of disk + gas-flow + boundary conditions of heat transfer which allows take into account gas heating and its influence on boundary conditions and disk temperature. Fig.4 demonstrates temperature distribution at beginning of the take-off regime.

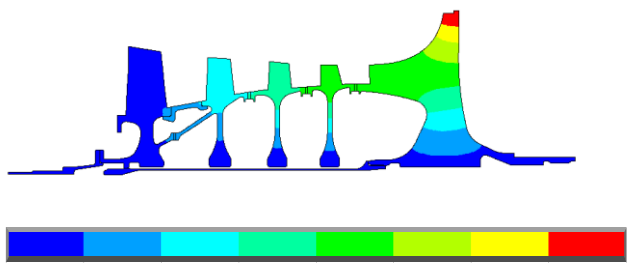


Fig. 4. Temperature distribution in rotor of 4+1 Prototype

2D axisymmetric structural analysis finite element calculations under given thermal conditions and RPM are resulted in detailed information on stresses (see Fig.5)

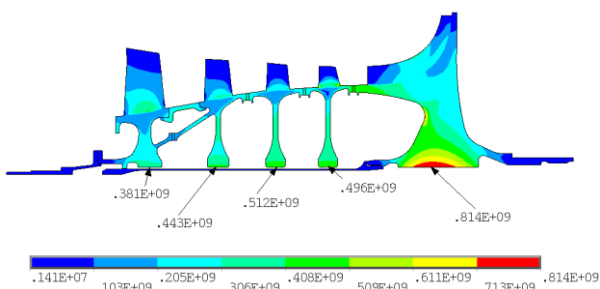


Fig. 5. Rotor disc equivalent stresses, Pa

Fig.5 shows that impeller disc is a critical part of compressor structure: maximum stress is observed in the bore of impeller disc and is equal to 814MPa. This is a rather high value. It confirms that beginning of take-off in the most dangerous flight regime.

Nevertheless, being designed following safe-life approach, the impeller’s disc has enough strength capacity (safety margin).

2.4 Performances of Compressor-Prototype

3D Navier-Stokes analysis in-house code was used to calculate the 4+1 Prototype performance maps at off-design speeds (see Fig.6) and to determine inlet guide vane turning (θ) schedule.

RPM	100%	94%	86%	80%	70%
θ	0°	15°	31°	40°	50°

In the calculations the rotor clearance-to-span ratio in the last stage of axial part is 1.5% and in the centrifugal impeller is 3.9%. All the axial stator vanes are cantilever.

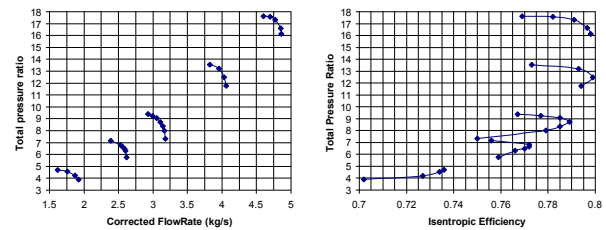


Fig. 6. Numerical Performances of the 4+1 Prototype

Fig.6 demonstrates satisfactory performances and surge margin (SM) of the prototype. Main features of the map of performances (namely, flow-rate, adiabatic efficiency and SM) are extended to all the compressors designed below. This is the main advantage of the “evolution of designs” adopted in this paper.

Parameters of axial part (Axial), centrifugal stage (Centrif) and whole Compressor-Prototype (Σ) are as follows:

$U_{R1tip} = 456$ m/s	Axial	Centrif	Σ
$U_{2imp} = 552$ m/s	stages	stage	
Pressure ratio PR	5.74	2.81	16.13
Adiabatic efficiency η_{ad}^*	0.847	0.798	0.798

2.5 Axial Part Tip Speed Limit

To increase power-to-weight ratio the compressor inlet annulus area has been increased to obtain a 25% enlargement of the flow-rate. For that axial blades were elongated 18% of their original heights but hub contour of the blades left unchanged (see Fig.7). In the case, all the disks remain as before, and weight of construction is almost invariant.

Increase of blade heights means increase of aspect ratio of blades and in the same time increase of tip speed (for the invariant RPM). It is interesting to note that these both events allow maintain SM.

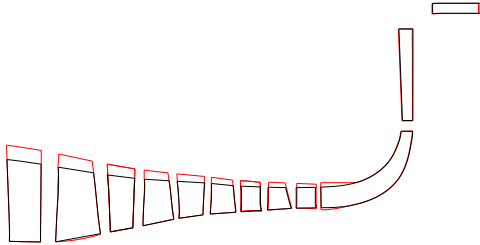


Fig. 7. Flow-paths of 4+1 Prototype (black lines) and 4+1 Axial Tip Speed Limit Compressor (red lines)

Corrected rotational speed at the periphery of the first stage rotor blade (Rotor1) equals to 493m/s. Here this high rotational speed is considered as limiting rotational speed for axial part of compressor (to exclude Rotor1 shock losses elevation). The hub-to-tip diameter ratio of Rotor1 is 0.534.

In this paper we develop a family of compressors. Axial parts of 3+1, 4+1 and 5+1 compressors are designed as having the same three front axial stages. In other words, the axial part of compressor 4+1 is obtained from the axial part of compressor 3+1 by addition of the fourth stage (with a corresponding displacement of the centrifugal stage). The same is true for the compressor 5+1. Each added stage is profiled so that it throttles the compressor in front of him at the same point on the characteristic, in which he worked without the added step. This means that the four front stages of axial portion of 5+1 compressor give the same parameters as the axial part of compressor 4+1. And three-stage axial inlet of the compressor 5+1 gives the same parameters as the three-stage axial inlet of the compressor 4+1 and axial part of the 3 + 1 compressor.

It should be noted that the level of the circumferential velocity is high enough to design the axial stage as compressor with a constant average diameter and thus achieve a high degree of pressure increase for moderate aerodynamic loading of axial stage. The hub-to-

tip diameter ratio at the outlet of the axial part of 5+1 compressor equals 0.856, so rear centrifugal stage can be designed with or without S-shaped transition duct.

The parameters of the axial part of compressor 5+1 are as follows:

$U_{Rtip} = 493 \text{ m/s}$	3 stages	4 stages	5 stages
PR	4.493	5.929	7.97
η_{ad}^*	0.858	0.852	0.846

2.6 Centrifugal Impeller Exit Tip Speed

The range of considered centrifugal impeller-exit tip speed lies between 529m/s and 593m/s. Fig.8 presents 4+1 compressor with limiting axial part (493m/s) and impeller (593m/s) tip speed velocities laid over the 4+1 Prototype with moderate axial part (456m/s) and impeller (553m/s) tip speed velocities.

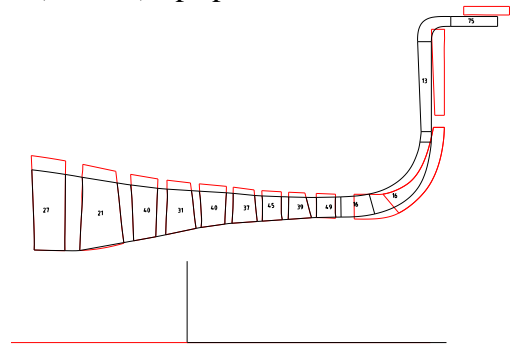


Fig. 8. Flow-paths of 4+1 Prototype (black) and 4+1 Axial Speed Tip Limit Impeller Tip Speed Limit (red)

Pressure ratio of centrifugal stage varies with corrected rotational speed determined by total pressure and temperature at the exit of axial part of compressor. Adiabatic efficiency of centrifugal stage depends on the impeller tip speed as follows (identical for 3+1, 4+1 and 5+1 compressors):

$U_{2imp} \text{ (m/s)}$	PR _{centrifugal stage}	$\eta_{ad}^* \text{ centrifugal stage}$
593	3.1 ÷ 3.4	0.800
553	2.6 ÷ 2.9	0.807
529	2.4 ÷ 2.6	0.814

3 3+1 Compressor

Compressor 3 + 1, which consists of three levels of axial and centrifugal closing

stages, has a potential to achieve PR=16. For that tip speed at the outlet of the centrifugal impeller has to be equal to $U_{2imp} = 593\text{m/s}$.

Impeller design has been considered in two variants: with S-shaped transition duct between axial part and centrifugal stage and without this transition channel. The flow-paths of the two compressors are shown in Figure 9: inclusion of the transition duct greatly increases the axial length of the compressor 3 + 1.

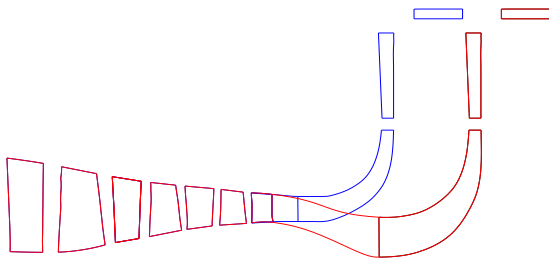


Fig. 9. Flow-paths of 3+1 Compressor with S-duct (red) and without it (blue)

Parameters of the axial part and the centrifugal stage without and with S-duct are shown below:

$U_{R1tip} = 493 \text{ m/s}$ $U_{2imp} = 593 \text{ m/s}$	Axial part w/o S-duct	Centrif stage	Σ
PR	4.84	3.25	15.75
η_{ad}^*	0.850	0.760	0.775

$U_{R1tip} = 493 \text{ m/s}$ $U_{2imp} = 593 \text{ m/s}$	Axial part with S-duct	Centrif stage	Σ
PR	4.76	3.30	15.72
η_{ad}^*	0.854	0.797	0.797

As is seen, application of the transition S-duct improves efficiency of the centrifugal stage by 3.7%. The reason is the difference in centrifugal impeller efficiency with S-duct and without it.

The fact is that in compressor 3+1 flow Mach number at the outlet of the axial part is large enough. As a result, within the blade-to-blade passage at the inlet of the centrifugal impeller without S-duct a supersonic flow zone (in relative motion) takes place.

S-duct lowers impeller tip radius, so rotational speed falls and causes subsonic flow

within blade-to-blade passage, resulting in reduced flow diffusion and increasing efficiency of impeller and centrifugal stage.

Note, in compressors 4+1 and 5+1 the phenomenon of impeller supersonic flow is absent, and from the standpoint of aerodynamics this transitional duct becomes superfluous. However, the duct may be useful to reduce the strength requirements for ovalization of compressor stator and misalignment of impeller and its shroud.

4 4+1 Compressor

Compressor 4+1, consisting of four axial stages and a centrifugal rear stage provides PR=16 at the impeller tip speed equal to $U_{2imp} = 553\text{m/s}$. This means that it is possible to compare aerodynamic parameters of the 4+1 compressor and the compressor 3+1 with S-duct. Flow-paths of the two compressors are shown in Fig.10.

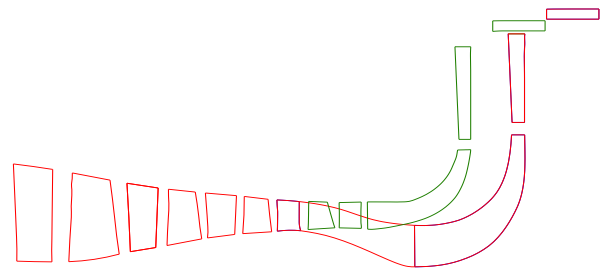


Fig. 10. Flow-paths of 3+1 Compressor with S-duct (red) and 4+1 (green) providing the same output PR

Parameters of the axial part and the centrifugal stage of 4+1 compressor are shown below:

$U_{R1tip} = 493 \text{ m/s}$ $U_{2imp} = 553 \text{ m/s}$	Axial part 4 stages	Centrif stage	Σ
PR	6.21	2.63	16.33
η_{ad}^*	0.848	0.808	0.805

Addition of the fourth axial stage reduces efficiency of axial part by 0.6%. But, 40m/s drop of U_{2imp} increases adiabatic efficiency of the centrifugal stage by 1%. Moreover, the redistribution of work between the axial part and the centrifugal stage increases

the axial part contribution to the whole compressor efficiency. As a result, adiabatic efficiency of the compressor 4+1 is higher than that of the compressor 3+1 by 0.8%.

Increase of impeller tip speed up to $U_{2imp} = 593\text{m/s}$ makes it possible to achieve $PR=20$:

$U_{R1tip} = 493\text{ m/s}$ $U_{2imp} = 593\text{ m/s}$	Axial part 4 stages	Centrif stage	Σ
PR	6.01	3.35	20.12
η_{ad}^*	0.855	0.798	0.798

i.e. adiabatic efficiency of the compressor 4+1 with $U_{2imp} = 593\text{ m/s}$ practically coincides with the efficiency of S-ducted compressor 3+1. Thus, addition of the fourth axial stage retains whole compressor efficiency, and considerably increases total pressure at its outlet.

5 5+1 Compressor

At the circumferential speed at the outlet of the centrifugal impeller equal to $U_{2imp}=553\text{m/s}$ compressor 5+1 produces total pressure ratio 21:

$U_{R1tip} = 493\text{ m/s}$ $U_{2imp} = 553\text{ m/s}$	Axial part 5 stages	Centrif stage	Σ
PR	7.77	2.681	20.84
η_{ad}^*	0.845	0.795	0.797

This $U_{2imp}=553\text{m/s}$ 5+1 compressor is comparable with $U_{2imp}=593\text{m/s}$ 4+1 compressor. Adiabatic efficiencies of those compressors is the same. Again, addition of the fifth axial stage retains whole compressor efficiency, and considerably increases total pressure at its outlet.

At $U_{2imp}=593\text{m/s}$ compressor 5+1 produces total pressure ratio 25:

$U_{R1tip} = 493\text{ m/s}$ $U_{2imp} = 593\text{ m/s}$	Axial part 5 stages	Centrif stage	Σ
PR	7.97	3.125	24.92
η_{ad}^*	0.846	0.796	0.794

$U_{2imp}=529\text{m/s}$ 5+1 compressor produces rather high total pressure ratio, which is again comparable with $U_{2imp}=593\text{m/s}$ 4+1 compressor. Fig. 11 presents flowpaths of these compressors.

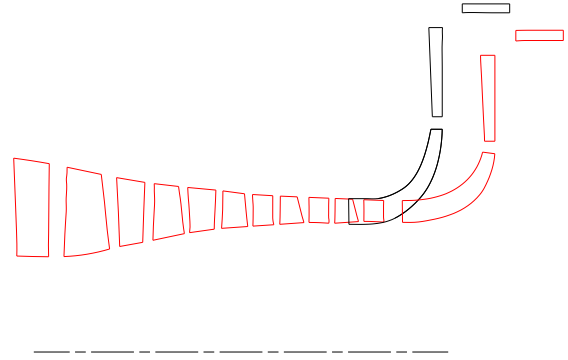


Fig. 11. Flow-paths of Compressors 4+1 (black) and 5+1 (red) providing the same output total pressure ratio

Parameters of the $U_{2imp}=529\text{m/s}$ 5+1 compressor are as follows:

$U_{R1tip} = 493\text{ m/s}$ $U_{2imp} = 529\text{ m/s}$	Axial part 5 stages	Centrif stage	Σ
PR	7.86	2.473	19.45
η_{ad}^*	0.846	0.811	0.807

6 Stress-strain state of 5+1 Compressor

To assess the feasibility of the compressor designs, analysis of the stress-strain state (SSS) of the compressor rotor 5+1 has been performed. Degree of 5+1 compression and outlet temperature are the highest (comparing with 3+1 and 4+1) even at low tip rotational speed of impeller ($U_{2imp}=529\text{m/s}$). 3D Navier-Stokes calculated flow temperature field was used to determine 5+1 rotor thermal state at the beginning and at the end of take-off.

Stress-strain calculations have been performed for the 5+1 rotor at two tip impeller rotational speeds $U_{2imp}=553\text{m/s}$ and 593m/s (corresponding to total pressure ratio $PR=21$ and 25) for existing material VT25 (titan-based alloy).

Generally, strained state calculations have shown that the largest axial displacements are located on the periphery of the disc of the centrifugal impeller (due to the flexural deformation of disk and blades). This observation is very important since the axial movement of the periphery of the impeller determines the change in the clearance gap

between the impeller and the shroud (cover). In the region impeller blade height is small, so any clearance gap variation influences the impeller adiabatic efficiency in a great manner.

equals to 0.643 mm. This is a rather large value which can cause rubbing of shroud by impeller' blades.

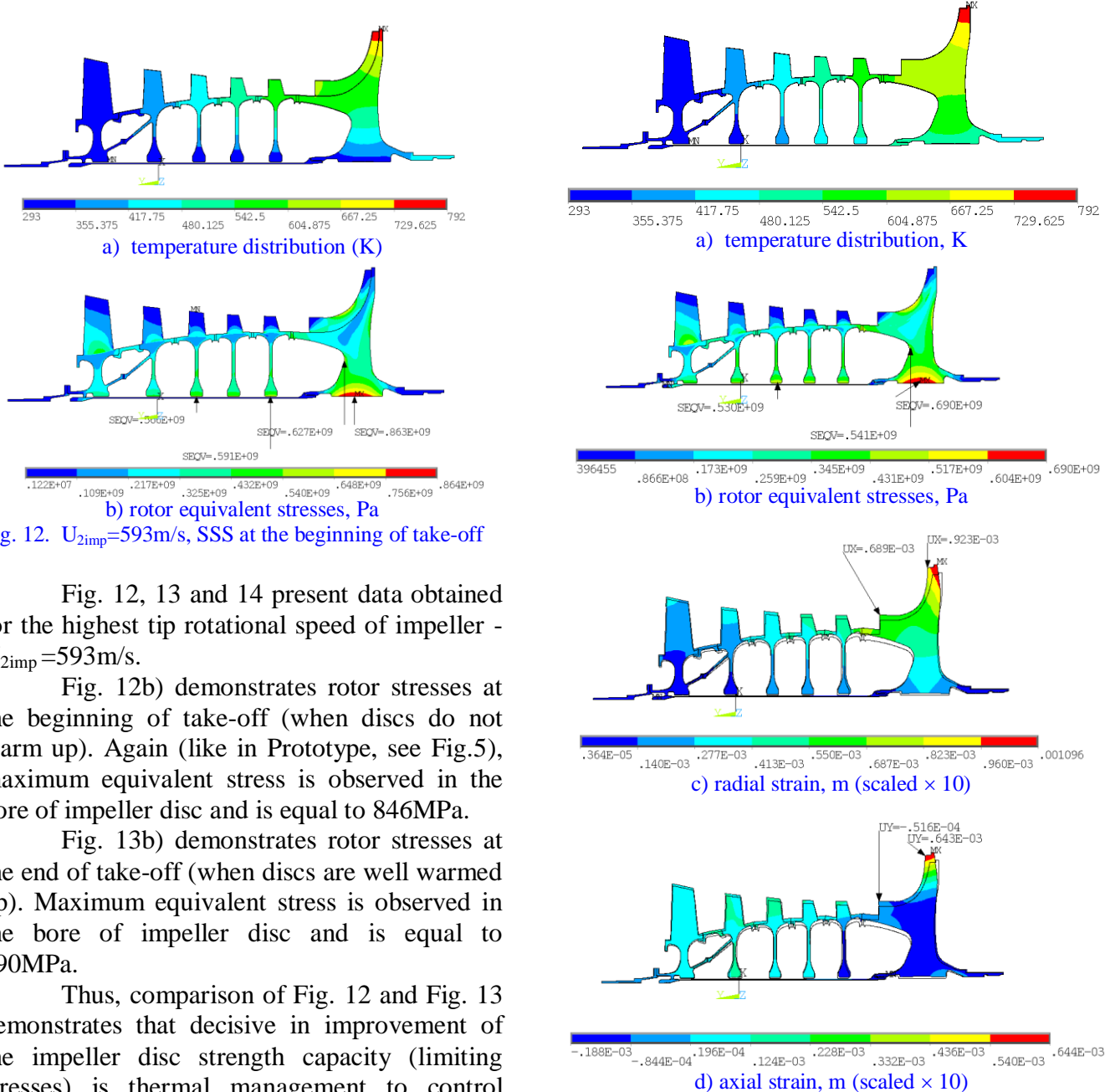


Fig. 12. $U_{2imp}=593\text{m/s}$, SSS at the beginning of take-off

Fig. 13. $U_{2imp}=593\text{m/s}$, SSS at the end of take-off

Fig. 12, 13 and 14 present data obtained for the highest tip rotational speed of impeller - $U_{2imp}=593\text{m/s}$.

Fig. 12b) demonstrates rotor stresses at the beginning of take-off (when discs do not warm up). Again (like in Prototype, see Fig.5), maximum equivalent stress is observed in the bore of impeller disc and is equal to 846MPa.

Fig. 13b) demonstrates rotor stresses at the end of take-off (when discs are well warmed up). Maximum equivalent stress is observed in the bore of impeller disc and is equal to 690MPa.

Thus, comparison of Fig. 12 and Fig. 13 demonstrates that decisive in improvement of the impeller disc strength capacity (limiting stresses) is thermal management to control distribution of temperature in centrifugal impeller disc. Obtained change of temperature distribution of centrifugal impeller can significantly smoothed by the blowing of warm air in the disc-to-disc cavity. This measure leads to an increase in the disk strength capacity (safety margin) up to 18%.

According to Fig. 13d) maximum axial strain of impeller is located on impeller tip and

Impeller disc has been varied to investigate sensitivity of strains to the disc shape. Impeller disc has been re-shaped to increase disc stiffness.

Fig.14 b) demonstrates rotor stresses at the end of take-off for the new shape of impeller disc. Maximum equivalent stress observed in

the bore of impeller disc is equal to 683MPa. It means that increase of stiffness provided by new disc does not improve the impeller's disc strength capacity.

According to Fig. 14d) maximum axial strain of impeller located on impeller tip equals to 0.003 mm. Thus increase of stiffness of the impeller's disc practically eliminates axial displacements at the tip of impeller and thus reduces the tip clearance change at the exit of impeller.

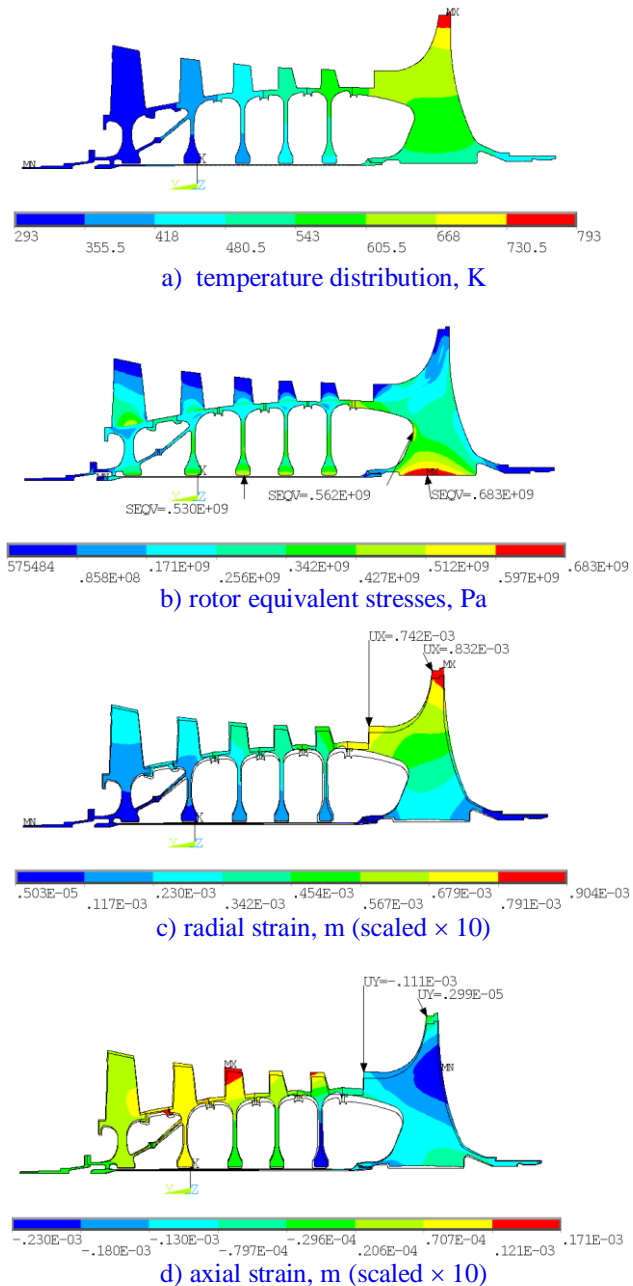


Fig. 14. $U_{2imp}=593m/s$, variation of the impeller disc, SSS at the end of take-off

It seems evident that diminishing of impeller tip rotational speed has to lower the level of stresses within impeller disc. Fig. 15 presents data for $U_{2imp} = 553 m/s$.

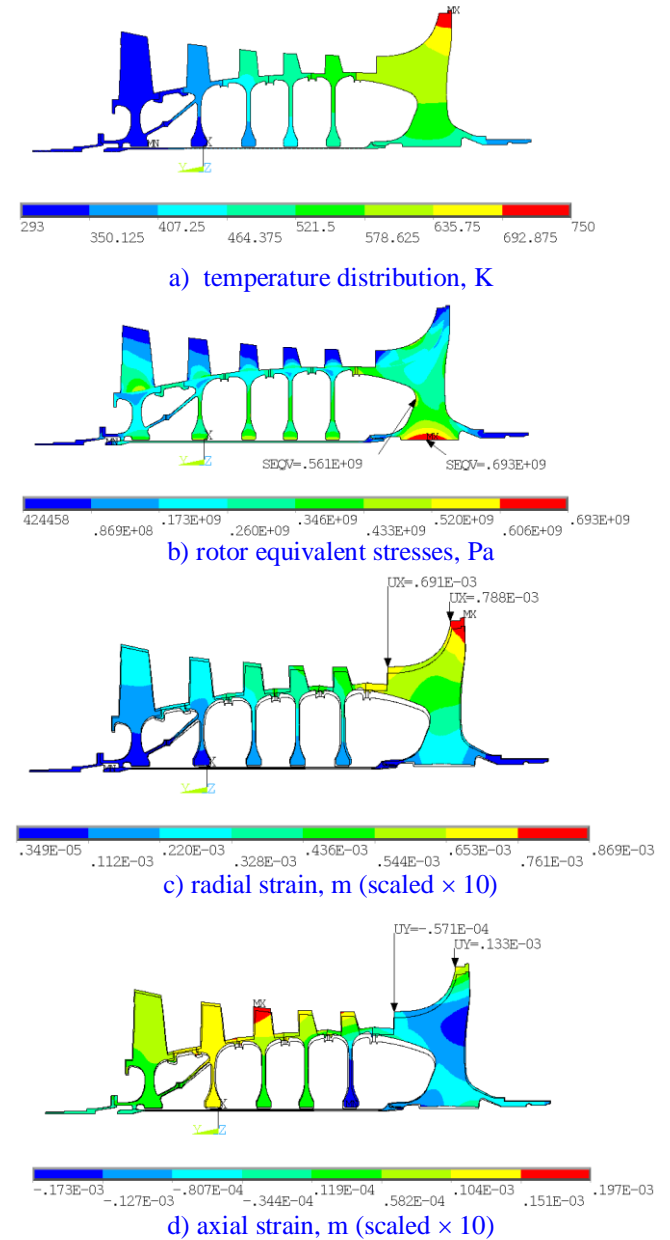


Fig. 15. $U_{2imp}=553m/s$, SSS at the end of take-off

Fig. 15b) demonstrates that maximum equivalent stress observed in the bore of impeller disc is equal to 693MPa. It means (being compared with Fig. 13b) that reduction of impeller tip rotation speed from 593m/s to 553m/s does not lead to a substantial increase in the impeller disc safety margin.

In the same time comparison of Fig. 15d), where axial strain of impeller tip equals to

0.133mm, and Fig. 13d) confirms that it is much easier to provide an acceptable level of the tip clearance variation in case of lower rotational speed.

Conclusion

This paper presents the aerodynamic and strength design of the family of axial-centrifugal compressors for a turboshaft engine producing increase of the total pressure in the range $PR = 16 \div 25$. This range of pressure ratio is a characteristic of modern and future small gas turbine engines.

High rotational speed of axial part ($U_{R1tip} = 493$ m/s) and centrifugal part (up to $U_{2imp} = 593$ m/s) of the axial-centrifugal compressors makes it possible to achieve this high PR in 4÷6 stages, thus family of compressors consists of 3+1, 4+1 and 5+1 compressors.

3D Navier-Stokes aerodynamic design of blades and rotor discs with the strength and technological limitations provided a high degree of reliability of the results for the entire family of compressors.

The principle of unification, which consists in the identity of the aerodynamic forms and flow fields used to create the new compressors led to the “evolutionary design” process and therefore provides predictable output. In particular, the family’s characteristic value of adiabatic efficiency is 0.798 and does not depend on the degree of pressure rise in the compressor and the number of stages. It is also due to correct choice of the compression work split between the axial part of compressor and the centrifugal stage

Features identified in the calculation of the stress-strain state of the compressors are included in the list of rules and restrictions on the aerodynamic design.

It is shown that construction of the family of compressors for considered range of parameters (pressure ratio and temperature) can be based on the existing material VT25 (titan-based alloy).

Copyright Statement

The authors confirm that they, and/or their company or organization, hold copyright on all of the original material included in this paper. The authors also confirm that they have obtained permission, from the copyright holder of any third party material included in this paper, to publish it as part of their paper. The authors confirm that they give permission, or have obtained permission from the copyright holder of this paper, for the publication and distribution of this paper as part of the ICAS proceedings or as individual off-prints from the proceedings.